

## RESEARCH ARTICLE

Accepted: 6 January 2018

# Critical analysis of line loadability constraints

Stefano Quaia 

Department of Engineering and Architecture, University of Trieste, Via Valerio, 10, Trieste 34127, Italy

**Correspondence**

Stefano Quaia, Department of Engineering and Architecture, University of Trieste, Via Valerio, 10, Trieste 34127, Italy.  
 Email: quaias@units.it

**Funding information**

Università degli Studi di Trieste, Grant/Award Number: Finanziamento di Ateneo FRA 2016

**Summary**

This paper develops a critical analysis of the constraints that influence the loadability curves of overhead transmission lines. The constraints considered are conductor thermal limit, allowed voltage drop (or voltage quality limit), steady-state (or angle) stability margin, voltage stability margin, and Joule losses limit. The analysis points out the different meanings and/or bearing of the various limits. In addition, the paper outlines a general comparison of voltage and angle stability and discusses the possible role of Joule losses, which are usually not included in line loadability analysis. The paper also discusses how line loadability is affected by the replacement of standard aluminium conductor steel reinforced conductors with high-temperature low-sag conductors and by reactive compensation with shunt reactors and series capacitors.

**KEYWORDS**

conductor thermal limit, high-temperature conductors, line loadability, power transmission, steady-state stability, voltage stability

## 1 | INTRODUCTION

The loadability curves are the graphic representation of the steady-state theoretical maximum power capability (measured at the receiving end) of overhead transmission lines (OHLs) as a function of the line length,  $L$ . They are largely independent from system-dependent constraints, like the N-1 contingency criterion, and transmission reliability margin. Therefore, these curves are a useful tool when attention is focused on the characteristics/performances of OHLs, without any reference to the surrounding power system.

The loadability curves were first derived empirically by St Clair,<sup>1</sup> on the basis of practical considerations and experience. Later, a theoretical basis for the St Clair loadability curves was developed in Dunlop et al.,<sup>2</sup> where the factors that influence the maximum permissible power are the overhead conductor thermal limit, the maximum permissible voltage drop ( $\Delta U_{\max}$ ), and the steady-state (or “angle”) stability.

---

**List of symbols and acronyms:** OHL, overhead transmission lines; HTLS, high-temperature low-sag;  $L$ , line length; ACSR, aluminium conductor steel reinforced; ACCC, aluminium conductor composite core;  $\Delta U_{\max}$ , maximum permissible voltage drop; SIL, surge impedance loading;  $I_{\text{th}}$ , current capacity at the thermal limit;  $U_1$ , sending end voltage (complex);  $U_2$ , receiving end voltage (complex);  $L_{\text{th}}$ , maximum line length for which the line loadability matches the thermal limit;  $I_2$ , line current at the receiving end (complex);  $\cos\varphi_2$ , power factor at the receiving end;  $A_1$ ,  $B_1$ , and  $C_1$ , auxiliary constants of the line (complex);  $K$ , line propagation constant (complex);  $Z_0$ , line surge impedance (complex);  $Z_1$ , line impedance (complex);  $R_1$ , line resistance;  $X_1$ , line reactance;  $x_1$ , per kilometre line reactance;  $U_S$  and  $U_R$ , complex voltages of the network equivalents at the two line ends;  $P_{\max}$ , steady-state stability limit;  $Z_{\text{load}}$ , load impedance (complex);  $\theta$ , angle of  $Z_1$ ;  $\varphi$ , angle of  $Z_{\text{load}}$ ;  $P_{\max,U}$ , voltage stability limit;  $U_{2,\text{critical}}$ , critical voltage at the receiving end;  $\Delta P_{\max}$ , Joule power losses; HVDC, high voltage direct current; HVAC, high voltage alternate current; SVC, static var compensators;  $X_{\text{SR}}$ , reactance of shunt reactor

Using the same methodologic approach, Kundur<sup>3</sup> reports the “universal loadability curve” of uncompensated OHLs applicable to all voltage levels. In fact, the per-unit (p.u.) line data normalized using the surge impedance loading and surge impedance is independent of line construction and voltage rating.

In these classical works, the theoretical maximum value of unity power factor ( $\cos\varphi = 1$ ) is assumed for power transmission. The effect on the loadability curves of actual, less-than-one power factor values was discussed thoroughly in Lauria et al,<sup>4,5</sup> in the frame of a comparative study among different OHLs solutions (both traditional and innovative). However, the line power factor is strongly influenced by the var supply capability available in the system. To this regard, the reader can refer to Kay et al,<sup>6</sup> where line loadability dependence on the actual var supply capability is investigated in detail, and to Gutman,<sup>7</sup> where shunt reactor compensation and voltage regulation are included in the analysis.

The effect on line loadability of further constraints relevant to voltage stability were analysed as well in a few papers.<sup>8,9</sup> Finally, in addition to the previous limiting factors, in Lauria et al,<sup>4,5</sup> a limit on the Joule power losses was considered too.

These various constraints determine different “regions” of the loadability curves (Figure 1). In the first region, the line loadability is determined by the conductor thermal limit. The extension of this region depends on several variables (conductors and line parameters, voltage drop limit  $\Delta U_{\max}$ , load power factor). To fix ideas, one can assume that the first region extends up to roughly 50 to 100 km.

In the second region, the permissible power is limited by the constraint  $\Delta U_{\max}$ . The second region is wide and can extend up to roughly 300 to 500 km or even more, depending again on several variables. As  $L$  increases, further regions correspond to other constraints relevant to line or system performance: the steady-state stability margin, the voltage stability margin, and/or the maximum Joule losses allowed along the line.

In this paper, the various constraints and their nature are analysed one by one, pointing out their different meanings and their possible connection with the parameters of the whole power system and showing that some of them can be temporarily exceeded if more global conditions are satisfied. A general comparison between angle and voltage stability is performed too, and the possible role of Joule losses in line loadability is discussed. In addition, the paper analyses how line loadability is affected by the replacement of standard aluminium conductor steel reinforced (ACSR) conductors with high-temperature low-sag (HTLS) conductors and points out the limits of this measure. The effects of reactive compensation with shunt reactors and series capacitors on the loadability curves are shortly discussed as well. Finally, a calculation example is reported and commented in the last section.

## 2 | CONDUCTOR THERMAL LIMIT

In OHLs, the current capacity at the thermal limit,  $I_{th}$ , is the maximum current that leads to acceptable values for

1. “risk of discharge,” ie, the probability of a discharge on the objects situated under or crossed by the OHL caused by the conductor sag due to the thermal expansion, and

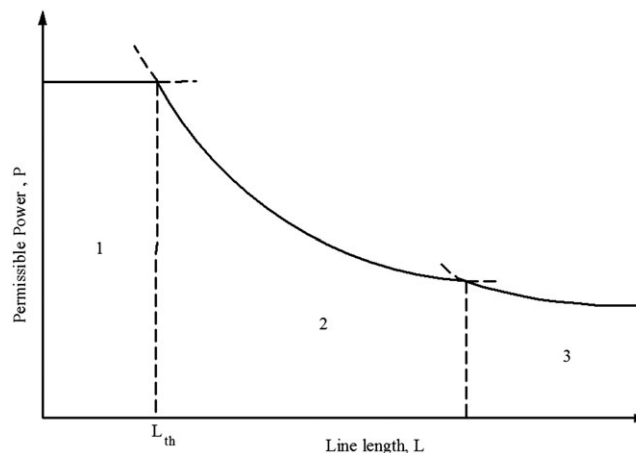


**FIGURE 1** Typical structure of transmission line loadability curve

**TABLE 1** Current capacities in temporary operation (from Italian Standard<sup>10</sup>)

% Probability	Annual Duration, h	Allowed Current Capacity in % of the Normal (Constant) Current Capacity $I_{th}$
Normal operation 96.7	8472	94
Temporary operation 3.2	280	113
Temporary operation 0.1	8	136
Normal operation 98.3	8612	73
Temporary operation 1.6	140	117
Temporary operation 0.1	8	146

- “conductor aging,” ie, the ageing of the conductor material (and also of joints and terminal blocks) due to temperatures higher than the design temperature. Conductor ageing is identified by the breaking load reduction (compared with the nominal breaking load) determined by the conductor's temperature through time.

The current capacity  $I_{th}$  depends on the characteristics of the conductors, on the line location and on the season, and is independent from the line length.

At the thermal limit, the power delivered at the receiving end is  $P_2 = \sqrt{3} U_2 I_{th} \cos\varphi_2$ . Assuming that the magnitude of the receiving end voltage  $U_2$  is constant, in the thermal limit region, the loadability curve relevant to a given  $\cos\varphi_2$  value is a horizontal segment (like reported in Figure 1). Conversely, if the sending end voltage magnitude  $U_1$  is assumed constant,  $U_2$  changes with the line load and the corresponding power is not simply proportional to  $I_{th}$  but depends on the voltage drop across the line.

However, if the power transported changes in time (as always happens), temporary overloads are allowed provided that the overall risk of discharge and conductor ageing are not increased. This means that the thermal limit is not an absolute limit, but it can be exceeded for short periods when necessary. For example, the Italian Standard CEI 11-60 allows to increase the current  $I_{th}$  for temporary operation.<sup>10</sup> In particular, this standard reports 2 (among infinite possible) operation modes with temporary overloads. Both of them are determined with reference to the risk of discharge, which is normally more restrictive than the conductor ageing. As Table 1 shows, each operation mode envisages 2 possible current capacities in temporary overload, expressed as a percentage of the current capacity in normal (constant current) operation. The allowed current capacity in normal operation is reduced (to 94% and 73%, respectively) to keep the overall risk of discharge unchanged. Of course, the temporary overload must be consistent with the system protections set-up.

The maximum line length for which the line loadability corresponds to the thermal limit,  $L_{th}$  (see Figure 1), depends on the following 3 variables:  $\Delta U_{max}$ ,  $\cos\varphi_2$ , and  $I_{th}$ .

$L_{th}$  increases with  $\Delta U_{max}$  and  $\cos\varphi_2$ , but  $L_{th}$  decreases if  $I_{th}$  increases. Therefore, increasing the conductor thermal limit will shorten the first region of the loadability curves. Considering the 400 kV OHLs widely used in Western Europe whose loadability curves are reported in the last section of this paper and taking  $I_{th} = 2038 \text{ A}^*$  and  $\Delta U_{max} = 5\%$ , simulations provide  $L_{th} = 115 \text{ km}$  with  $\cos\varphi_2 = 1$  and  $L_{th} = 57 \text{ km}$  with  $\cos\varphi_2 = 0.97$ . If we take  $I_{th} = 2952 \text{ A}^\dagger$  and  $\cos\varphi_2 = 0.97$ ,  $L_{th}$  reduces to just 38 km.

The thermal limit can be drastically increased using HTLS conductors.<sup>11-13</sup> High-temperature low-sag conductors can either equip new lines or replace the traditional ACSR conductors in existing lines (line “reconductoring”). Aluminium conductor steel reinforced conductors, characterized by strands of aluminium wrapped around steel cables, have been traditionally used for a long time in transmission OHLs. A first type of HTLS conductor is the Aluminium Conductor Composite Core (ACCC) in which a hybrid carbon and glass fibre core characterized by low coefficient of thermal expansion replaces the steel core strands of ACSR conductors. The carbon fibre composite core is up to 25% stronger than the steel core, which significantly reduces the sag of ACCC conductors at high temperatures. Additionally, since the carbon fibre composite core is lighter than steel, ACCC conductors can be lighter than ACSR conductors. This allows longer spans and fewer and shorter supporting structures, reducing the capital costs of OHLs. Otherwise, resorting to trapezoidal shaped aluminium wires, ACCC conductors can incorporate more (up to 28%) aluminium without a weight or

\*According to the Italian Standard,<sup>10</sup> this is the thermal limit of the  $3 \times 585 \text{ mm}^2$  standard ACSR conductor bundle widely used in 400 kV OHLs in Northern Italy and during the hot season.

†Thermal limit of the  $3 \times 585 \text{ mm}^2$  standard ACSR conductor bundle in Southern Italy and during the cold season.

diameter increase, reducing electrical resistance, and thus, Joule losses at equal loading (up to 35% reduction). Overall, greater aluminium section and lower coefficient of thermal expansion allow to carry much more current (up to nearly twice) than a conventional ACSR conductor with the same size and weight. The main disadvantage of these conductors is the higher cost compared to ACSR conductors.

Another type of HTLS conductors is the gap conductors, consisting of layers of trapezoidal shaped, temperature-resistant aluminium-zirconium wires around a high-strength steel core. To allow the aluminium wires to move freely over the core, the outer diameter of the core is smaller than the inner diameter of the innermost layer of aluminium-zirconium wires. This gap becomes an essential part of the conductor and gives the conductor its special characteristics. Gap conductors, too, can carry much more current than the conventional ACSR conductors.

However, the increased thermal limit allowed by HTLS conductors can be exploited only in short lines, because for  $L > L_{th}$  (ie, in the second region of the loadability curves) the maximum voltage drop  $\Delta U_{max}$  becomes more restrictive than the thermal limit.<sup>14</sup> From this point of view, the maximum line length compatible with the use of HTLS conductors could be increased managing the voltage drop across the line through controlled var injection at the receiving end.<sup>15</sup>

A limitation to the current increase is posed by the right of way of the line, which depends on the magnetic induction limits imposed by laws and increases with the current capacity of the line. While in a new line equipped with HTLS conductors, the right of way is calculated at the project stage, in case of reconductoring the original right of way increases. Accordingly, complex and/or expensive changes to the line layout may be required to exploit HTLS conductors; otherwise, the current capacity increase may remain only a “potential” advantage.

### 3 | MAXIMUM VOLTAGE DROP (VOLTAGE QUALITY LIMIT)

The maximum voltage drop allowed across the line,  $\Delta U_{max}$ , is a constraint that concerns voltage regulation in the power system. An effective voltage regulation is required at each moment. Therefore, once the limit  $\Delta U_{max}$  has been fixed, it should never be exceeded (unlike the thermal limit discussed above).

In most papers,  $\Delta U_{max} = 5\%$  is considered the value that “adequately represents the condition of a line carrying heavy, but permissible, load without encountering unusual operating problems.”<sup>2</sup> Of course,  $\Delta U_{max} = 5\%$  is not a mandatory value, but it is reasonable assuming that any deviation from it should be limited. Lower values (eg,  $\Delta U_{max} = 4\%$ ) penalize line loadability, whereas higher values (eg,  $\Delta U_{max} = 6\%$ ) increase loadability but worsen voltage regulation and its effects on the quality of the power supply.

For analytical studies and computer simulations, the voltage drop across the line should be calculated using the complete line model with distributed parameters. Simpler models (shunt admittance neglected, lumped parameters, lossless line) introduce errors that increase with the line length. Considering that the voltage quality limit affects line loadability up to considerable line lengths, simplified line models and approximations should be avoided or carefully weighed. According to the complete line model, the voltage drop is

$$\Delta U = |U_1| - |U_2| = |A_1 U_2 + \sqrt{3} B_1 I_2| - |U_2|, \quad (1)$$

where  $U_1$  and  $U_2$  are the (complex) voltages at the sending and receiving ends,  $A_1$  and  $B_1$  the (complex) auxiliary constants of the line ( $A_1 = \cosh(KL)$ ;  $B_1 = Z_0 \sinh(KL)$  being  $K$  the propagation constant and  $Z_0$  the characteristic impedance of the line), and  $I_2$  the (complex) current at the receiving end. Said  $P_2$  and  $Q_2$  the active and reactive load power, the magnitude  $I_2$  is

$$I_2 = \frac{\sqrt{P_2^2 + Q_2^2}}{\sqrt{3} U_2} = \frac{P_2 \sqrt{1 + (\tan^2 \phi)}}{\sqrt{3} U_2}. \quad (2)$$

The approximated equation  $\Delta U = \sqrt{3} (R_1 I \cos \phi_2 + X_1 I \sin \phi_2)$  that can be used for short lines has the merit to highlight the strong dependence of the voltage drop on the load power factor. Of course, OHLs loadability decreases when the power factor decreases.<sup>4,5</sup> Note that negative values of  $Q$  (capacitive loads) increase the line loadability.<sup>14</sup> This is because the second term  $X_1 I \sin \phi_2$  becomes negative and the voltage drop reduces, as the Perrine-Baum diagram of the line illustrates.

In case of line reconductoring with HTLS conductors, in the second region of the loadability curves the higher thermal limit cannot be exploited. However, ACCC conductors with trapezoidal aluminium wires have, the outer diameter being equal, lower resistance than ACSR conductors, and thus, allow to get a small loadability increase as a consequence of a small voltage drop reduction.<sup>14</sup>

## 4 | STEADY STATE STABILITY

Stability constraints limit the risk of instability following random events (faults, disturbances, load/generation rapid changes).

The constraint relevant to the steady-state stability is commonly expressed through the (minimum) steady-state stability margin, or the corresponding (maximum) power angle. There is a difference in principle between the stability margin and the constraints discussed in the previous sections. While the thermal limit concerns the line parameters and geographical location and the voltage drop depends on the line parameters and loading, the steady-state stability does not concern the line alone but also involves features of the power system. Indeed, the calculation of the power angle involves the equivalent system reactances (or the short circuit power levels) at both line ends (Figure 2). Therefore, matching the steady-state stability constraint depends on the whole line + power system. This makes the steady-state stability constraint a system-dependent constraint to some degree.

For a given OHL, the stronger the power system, the lower the system reactances and their impact on the line loadability. Typical short circuit power levels range from 12.5 kA for a “weak” transmission system to 50 kA for a “well-developed” system.

In what follows,  $U_S$  and  $U_R$  stand for the constant (complex) voltages of the network equivalents at the 2 line ends,  $A'$  and  $B'$  the (complex) auxiliary constants of the system line + equivalent network reactances shown in Figure 1,  $\alpha$  the angle of  $A'$ ,  $\beta$  the angle of  $B'$ ,  $\delta$  the angle between  $U_S$  and  $U_R$ . By definition, the steady-state stability limit is the maximum value that the power at the receiving end  $P_R(\delta)$  can assume and corresponds to  $\delta = \beta$ :

$$P_{\max} = \frac{U_S U_R}{B'} - \frac{A' U_R^2}{B'} \cos(\beta - \alpha). \quad (3)$$

In a lossless system,  $B' = jX$  with  $X = X_S + X_1 + X_R$ ,  $\alpha = 0$ ,  $\beta = 90^\circ$  and (3) turns to the simpler (and often used) equation:

$$P_{\max} = \frac{U_S U_R}{X}, \quad (4)$$

which corresponds to the power angle  $\delta = 90^\circ$ .

An  $x\%$  stability margin means that the power transported at the receiving end of the line,  $P_2$ , must not exceed  $(100-x)\%$  of  $P_{\max}$ . Line loadability studies usually assume a 30% stability margin, which means that the (maximum) allowed power is 70% of the steady-state stability limit. This corresponds to about a  $44^\circ$  power angle.<sup>3</sup> Such margin is generally considered a suitable “reserve” to provide for stable system operation after a variety of “credible” contingencies which may increase a given line loading. Such changes in loading may be caused by temporary faults, loss of generation, and line switching. Of course, a higher stability margin will penalize line loadability.

Under the usual assumptions, the angle stability constraint prevails on the voltage quality limit for long lines. According to previous works,<sup>1-3</sup> steady-state stability can affect the line loadability starting from roughly  $L = 320$  km. However, the border length between the second and third region of the loadability curves can be much greater. If we refer to the 400 kV OHLs with standard  $3 \times 585 \text{ mm}^2$  ACSR conductors, intensive simulations performed in Lauria et al<sup>4,5</sup> show that, for  $L \leq 500$  km, the angle stability never becomes the actual limiting factor. For lines longer than 500 km, the system strength has only a moderate effect on the border length. For example, taking  $U = 400$  kV, the line reactance  $x_1 = 0.271 \text{ } \Omega/\text{km}$  and 25 kA short circuit power level at both ends, for  $L = 500$  km the overall line reactance  $X_1$  is 88% of the total reactance  $X$  which figures in 4.

Some papers have investigated the transient stability limits which ensure generators stability in case of temporary faults on OHLs close to a power plant. For example, referring to a line linking a power plant with the bulk power system, Lauria et al<sup>16</sup> investigate the transient stability limits resorting to the equal area criterion (ie, using a traditional deterministic approach based on the “worst case” analysis). In case of three-phase faults, the results show that the transient stability limits become extremely stringent, drastically reducing the line loadability. However, since three-phase faults

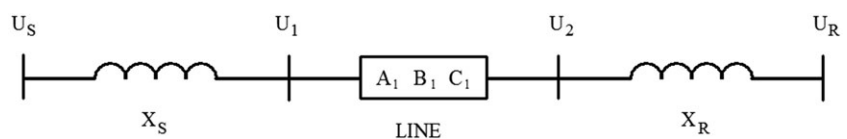


**FIGURE 2** Equivalent circuit for steady-state stability evaluation

are improbable and the impact on generators stability of (much more probable) single phase to ground faults is reduced by the single-phase opening of circuit breakers, overall, the above reported 30% steady-state stability margin can be generally considered an adequate stability constraint.

It is important to point out that a different approach to stability analysis, based on probabilistic techniques and motivated by the random nature of several variables involved, is adopted in various papers.<sup>17-22</sup> An exhaustive account of this topic can be found in Anders,<sup>23</sup> where the author states that “stability analysis is basically a probabilistic rather than a deterministic problem.” Accordingly, any angle stability constraints should not be considered as absolute limits but could be temporarily exceeded (similarly to what was said above concerning the thermal limit) provided that the overall risk of instability is adequately limited.

In case of line reconductoring, ACCC conductors have practically the same reactance of ACSR conductors, and thus, no practical loadability change is produced.

## 5 | VOLTAGE STABILITY

In addition to the previous constraints, which can be called “traditional” since for a long time they were considered the main constraints in line loadability, a few papers also analyse the limits posed to line loadability by voltage stability.<sup>8,9</sup>

Voltage stability basically depends on the relationships between P, Q, and U. Assuming the magnitude of the sending end voltage  $U_1$  as constant, the power transmitted reaches its maximum  $P_{\max}$  when the line series impedance  $Z_l$  and the load impedance  $Z_{\text{load}}$  have equal magnitude ( $Z_l/Z_{\text{load}} = 1$ ). In practice, this condition could be obtained in the case of very long lines (large  $Z_l$ ) and very high loads (small  $Z_{\text{load}}$ ). Using the simplest line model, lossless and without capacitance ( $Z_l = jX_l$ ), and assuming  $\cos\varphi_2 = 1$ , the voltage stability limit,  $P_{\max,U}$ , is

$$P_{\max,U} = \frac{U_1^2}{2X_l}. \quad (5)$$

The corresponding “critical” voltage at the receiving end is

$$U_{2,\text{critical}} = \frac{U_1}{\sqrt{2}}. \quad (6)$$

In a more general case, still neglecting the line capacitance and denoting by  $\theta$  and  $\varphi$  the angles of  $Z_l$  and  $Z_{\text{load}}$ , respectively, 5 and 6 become

$$P_{\max,U} = \frac{U_1^2}{2Z_l} \frac{\cos\varphi}{1 + \cos(\theta - \varphi)}, \quad (7)$$

$$U_{2,\text{critical}} = \frac{U_1}{\sqrt{2[1 + \cos(\theta - \varphi)]}}. \quad (8)$$

As it is known, the load power factor has a strong influence on voltage stability, and the voltage stability limit drastically increases (likewise the voltage drop reduces) passing from lagging  $\cos\varphi_2$  values to unity power factor and to capacitive (leading) power factors.

Unlike the steady-state stability limit expressed by 3 or 4, the voltage stability limit given by 5 or 7 depends only on the line parameters and line loading, and thus, is not system-dependent. However, this is true only if  $U_1$  can be assumed constant. Otherwise, a network equivalent impedance must be introduced upstream of the line, like we do for the angle stability analysis, making the voltage stability limit system-dependent too.

A comparison between angle stability and voltage stability is performed in Hao and Xu<sup>8</sup> where, however, the analysis is limited to the ideal case  $\cos\varphi_2 = 1$ . Taking as constraints the usual 30% steady-state stability margin and a 5% voltage stability margin (ie, the maximum power allowed is  $0.95 P_{\max,U}$ ), the conclusion is that the voltage stability can be more restrictive than the angle stability. But the question is can the voltage stability margin also be more restrictive than the voltage quality limit, thus affecting line loadability?

To answer this question, we must consider, on the one hand, that transmission lines exhibit a “voltage drop inversion” or “voltage rise effect,” consisting in the reduction of the voltage drop when L increases, at a constant load. This leads to a

certain increase of the loadability curves (ie, the derivative  $dP/dL$  becomes positive—see Figure 3 in Section 8) starting from a critical length.<sup>4</sup> This phenomenon reduces the effect of the voltage drop limit on the loadability curves, thus leaving “more space” to the other constraints and leading<sup>8</sup> to conclude that voltage stability can really affect OHLs loadability.

On the other hand, in a realistic power factor range (we can assume  $0.95 \text{ lagging} \leq \cos\varphi_2 \leq 1$ ), the voltage stability limit corresponds to very low critical voltages at the receiving end—according to 8, less than 0.7 p.u.—which are far beyond the voltage drop limit. Simulations performed demonstrate that the critical voltage increases with  $L$ . Assuming a 5% voltage stability margin, the corresponding receiving end voltage (which likewise increases with  $L$ ) is still beyond the 5% voltage quality limit until at least  $L = 600$  km. This prevents voltage stability from affecting the line loadability, unless very long lines are considered.

Going deeper in this matter, we note that the voltage rise effect is particularly evident at low-load conditions, but it is less evident at high loads and depends strongly on the load power factor. Taking  $\cos\varphi_2 = 1$  as made in Hao and Xu<sup>8</sup> and referring to the 400 kV OHLs already considered, simulations show that at the power corresponding to the voltage drop limit ( $\Delta U\% = 5\%$ ), the voltage rise effect is apparent only in extremely long lines ( $L > 750$  km). For lower values of  $\cos\varphi_2$ , the critical length for voltage drop inversion reduces (it is roughly 400 km for  $\cos\varphi_2 = 0.97$ ), but the power corresponding to the voltage drop limit reduces as well (in practice, this power is the loadability limit). This means that the ratio  $Z_1/Z_{\text{load}}$  reduces, preventing voltage instability.

Long lines need shunt reactors for reactive compensation. Shunt reactors do not affect line loadability, since they are usually removed under high load conditions. If they are permanently connected, their effect is to increase the voltage drop, preventing the voltage drop inversion and causing a right shift of the border between the second and the third region of the loadability curves.

These considerations lead to the conclusion that voltage stability cannot really affect the line loadability, unless extremely long lines are concerned and greater voltage stability margins and/or smaller steady-state stability margins are adopted.

Reconductoring has small effect on voltage stability. A certain reduction of the line resistance causes  $\theta$  to increase. According to 7 and 8, both the voltage stability limit and the critical voltage will slightly increase.

## 6 | JOULE LOSSES

In Lauria et al,<sup>4,5</sup> in the frame of a technical comparison among different solutions for transmission lines, Joule power losses ( $\Delta P_{\text{max}}$ ) are considered as a further technical aspect that could affect line loadability. The comparison includes HVDC lines for which, being the voltage drop smaller and in the absence of stability problems, Joule losses assume greater importance than in HVAC lines. In those papers, the same percent limit for Joule power losses and voltage drop ( $\Delta P_{\text{max}} = \Delta U_{\text{max}} = 5\%$ ) is assumed.

At the loadability limit (ie, at the maximum permissible power), simulations performed show that the ratio between percent power losses ( $\Delta P_{\text{max}}$ ) and percent voltage drop ( $\Delta U_{\text{max}}$ ) tends to increase with  $L$  and with the load power factor. Anyway, for line lengths up to more than 500 km and power factors in the range between 0.95 (lagging) and 1, at the loadability limit percent power losses are always less than the percent voltage drop ( $\Delta P_{\text{max}} < \Delta U_{\text{max}}$ ).<sup>4,5</sup> Only for longer lines, percent power losses can exceed percent voltage drop, see the example reported in Section 8.

Also, St Clair<sup>1</sup> took Joule losses into consideration, stating that they are largely an economic problem rather than a distinct limiting factor in line loadability. Therefore, any limit concerning Joule losses should involve the lost energy (annual, monthly, weekly, etc) rather than the instantaneous power losses. Thus, in the frame of normally changing line loading, an additional performance limit can concern the lost energy (or the average value of power losses), whereas setting a limit on the instantaneous power losses has scarce practical meaning. Note that these considerations are similar to those made in Section 2 speaking of the conductor thermal limit.

All things considered, Joule losses may have scarce importance for the loadability of HVAC OHLs.<sup>‡</sup> This importance is further reduced in case of reconductoring with HTLS conductors characterized by lower resistance than ACSR conductors (being the outer diameter equal).

<sup>‡</sup>The case of HVDC lines is different: For them, setting the same percent limit for both Joule power losses and voltage drop, one can easily verify that the power losses limit is always more restrictive than the voltage drop limit. Thus, Joule losses can be considered an important limiting factor for HVDC line loadability.<sup>4</sup>

## 7 | REACTIVE COMPENSATION

Shunt reactors are commonly installed on long transmission lines for voltage control<sup>§</sup> (see for instance, among several papers,<sup>7,24-26</sup>). Shunt reactors absorb reactive power and reduce overvoltages (Ferranti effect) at light load conditions. They also reduce overvoltages due to switching and lightning surges. Clearly, shunt reactors do not change the conductor thermal limit, nor the series reactances which play a major role in angle and voltage stability, but they change both voltage drop and Joule losses. However, if shunt reactors are removed under high load conditions, they have no effect on the line loadability. In the less common case of shunt reactors permanently connected to the line ends, said  $X_{SR}$  the reactance of each shunt reactor, the (complex) auxiliary constants  $A''$  and  $B''$  of the system line + reactors are given by

$$A'' = A_l + \frac{B_l}{jX_{SR}}, \quad (9)$$

$$B'' = B_l. \quad (10)$$

One can easily check that the effect is a considerable increase of the voltage drop under high loading, making the voltage drop limit more restrictive, and thus, reducing the line loadability.

In some cases, series capacitors are connected on OHLs. Series compensation, much less frequent than shunt compensation, reduces the overall line reactance (complete compensation is never considered: usually the compensation range is between 20% and 70% of the line reactance) and, therefore, is used to improve stability (both angle and voltage stability). As the voltage drop is reduced as well, series compensation has a considerable effect on line loadability.<sup>24</sup> The thermal limit region broadens ( $L_{th}$  increases), and in the following regions, the permissible power increases. However, series compensation is technically less simple and economically more expensive than shunt compensation. Attention must be paid to the increase of short circuit currents, to avoid possible subsynchronous resonance, and to the setting and coordination of the distance protections, whose operation is based on the measure of the line impedance.

## 8 | CALCULATION EXAMPLE

We refer here to the traditional (uncompensated) 400 kV three-phase OHLs widely used in Western Europe, equipped with the standard triple-core ACSR conductor bundles of  $3 \times 585 \text{ mm}^2$  cross section, already mentioned above.

The primary line constants are  $r = 0.021 \text{ } \Omega/\text{km}$ ,  $x = 0.271 \text{ } \Omega/\text{km}$ ,  $g = 4 \cdot 10^{-9} \text{ S/km}$ ,  $b = 4.21 \cdot 10^{-6} \text{ S/km}$ , which yield a surge impedance  $Z_0 = 257.4 \text{ } \Omega$  and a surge impedance level  $P_0 = 620 \text{ MW}$ .

The relevant loadability curves were calculated considering all the constraints discussed in the previous sections, namely, conductor thermal limit, voltage drop limit,  $\Delta U_{\max}$ , power losses limit,  $\Delta P_{\max}$ , steady-state stability margin, and voltage stability margin.

For these constraints, we assumed the following values: conductor thermal limit  $I_{th} = 2038 \text{ A}$  (see Section 2),  $\Delta U_{\max} = \Delta P_{\max} = 5\%$ , 30% steady-state stability margin and 50 kA short circuit level at both line ends, as in Kundur,<sup>3</sup> and 5% voltage stability margin. Figure 3 reports the loadability curves relevant to different power factors at the receiving end,  $\cos\varphi_2$ , in the range 0.97 to 1 (practical values for  $\cos\varphi_2$  can be assumed not less than 0.97, which corresponds to  $Q_2 = 0.25P_2$ ).

Figure 3 shows that the second region of the loadability curves extends up to more than  $L = 600 \text{ km}$ , exception made for the case  $\cos\varphi_2 = 1$ , for which the third region starts at  $L = 586 \text{ km}$ . Figure 4 shows that the constraint that affects the loadability curve after  $L = 586 \text{ km}$ , becoming more stringent than the voltage drop limit, is the Joule losses limit  $\Delta P_{\max}$ .

For these lines and with the assumed values of the constraints, both angle and voltage stability affect the loadability curves only at longer lengths. However, even if some OHLs longer than 600 km do exist in the world, the large majority of OHLs are by far shorter. For example, in Italy, the longest 400 kV transmission line is less than 300 km long.

In Figure 3, note also

1. the dependence of the loadability curves on the load power factor. Of course, this dependence is particularly strong in the voltage drop region;

<sup>§</sup>Less frequently, active compensators like synchronous condensers and static var compensators (SVC) are used instead of (passive) shunt reactors.



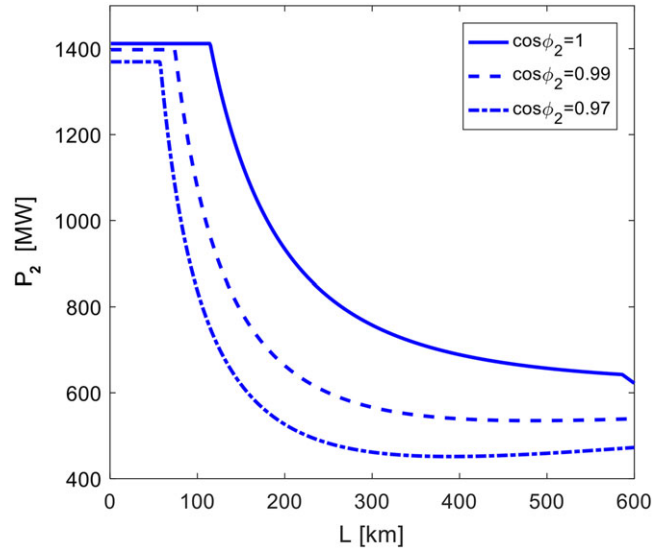


**FIGURE 3** Loadability curves of standard 400 kV overhead transmission lines

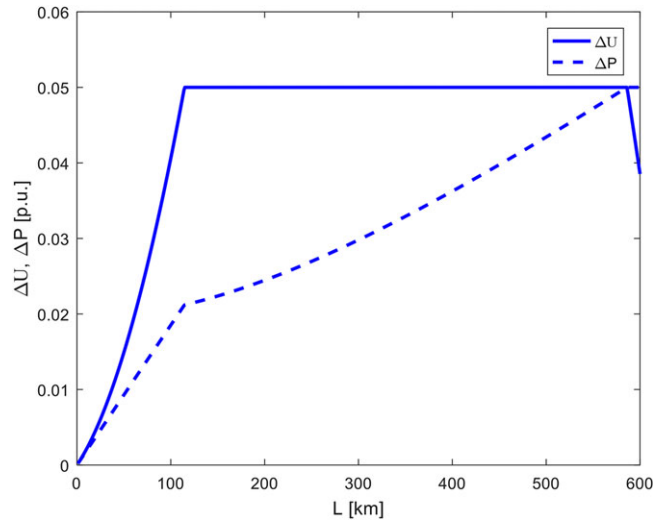


**FIGURE 4** Voltage drop and Joule losses at the loadability limit in the case  $\cos\phi_2 = 1$

2. the strong dependence of  $L_{th}$  on the load power factor (see the data reported in Section 2);
3. the voltage rise effect, evident in the curve relevant to  $\cos\phi_2 = 0.97$ .

Examining Figure 3, the reader can also imagine how the first region will narrow as the conductor thermal limit increases. A typical case is the substitution of ACSR conductors with HTLS conductors. In this case, the narrowing of the first region reduces the range of line lengths in which HTLS conductors can be fully exploited.

Another case of thermal limit increase is the temporary overload discussed in Section 2.

## 9 | CONCLUSIONS

In-depth analysis of the constraints that can affect OHLs loadability leads to interesting insights. When, as it always happens, the line load changes during time, the thermal limit is not an absolute limit but, provided that the overall risk of discharge is not increased, temporary overloads are allowed. This possibility can be exploited to get a temporary loadability increase in relatively short lines. Moreover, since stability can be regarded a probabilistic rather than

deterministic problem, also the stability limits (concerning both angle and voltage stability) could be exceeded for limited periods of time. This possibility can be exploited to get a temporary loadability increase in long lines. On the contrary, the voltage drop limit should never be exceeded, as this would worsen the quality of the power supply.

As to Joule losses, the calculation example demonstrates that setting a limit on the power losses could really affect the loadability of long lines. However, a more practical limit on the energy losses could hardly have the same effect.

A similar conclusion holds for the voltage stability margin, which is unlikely to prevail over the angle stability margin.

The much higher thermal limit of HTLS conductors, compared with traditional ACSR conductors, allows to increase the line loadability in the first region, whose width however considerably reduces, whereas in the following regions, the permissible power keeps roughly unchanged.

Concerning reactive compensation, removable shunt reactors have no effect on line loadability, and permanent shunt reactors reduce line loadability in the second region because of the increased voltage drop under high loads. On the contrary, series capacitors can considerably increase the line loadability starting from the voltage drop region.

Interesting directions for future research on these topics are

1. exhaustive exploration of the possible effects of voltage stability: the study should pinpoint the conditions that could make voltage stability an actual limiting factor for power transmission;
2. exploration of the possible effects of limiting Joule energy losses;
3. derivation of new loadability curves corresponding to the (temporary) relaxation of thermal limit and stability margins, according to a well-grounded risk analysis.

## ACKNOWLEDGEMENT

This work was financially supported by the Università degli Studi di Trieste—Finanziamento di Ateneo per progetti di ricerca scientifica—FRA 2016.

## ORCID

Stefano Quaia  <http://orcid.org/0000-0003-1717-750X>

## REFERENCES

1. St. Clair HP. Practical concepts in capability and performance of transmission line. Proc AIEE Pacific General Meeting, Vancouver, B.C., Canada, 1-4 September 1953.
2. Dunlop RD, R. Gutman R, Marchenko PP Analytical development of loadability characteristics for EHV and UHV transmission lines. *IEEE Trans PAS*, 1979;98(2):606-613.
3. Kundur P. *Power System Stability and Control. the EPRI Power System Engineering Series*. McGraw-Hill; 1994:228-230.
4. Lauria D, Mazzanti G, Quaia S. The loadability of overhead transmission lines. Part I: analysis of single-circuits. *IEEE Trans Power Deliv*. 2014;29(1):29-37.
5. Lauria D, Mazzanti G, Quaia S. The loadability of overhead transmission lines. Part II: analysis of double-circuits and overall comparison. *IEEE Trans Power Deliv*. 2014;29(2):518-524.
6. Kay TW, Sauer PW, Smith RA. EHV and UHV line loadability dependence on VAR supply capability. *IEEE Trans Power Apparatus Syst*. 1982;101:3568-3575.
7. Gutman R. Application of line loadability concepts to operating studies. *IEEE Trans Power Syst*. 1988;3(4):1426-1433.
8. Hao J, Xu W. Extended transmission line loadability curve by including voltage stability constrains. *IEEE Electrical Power & Energy Conference*, 2008:1-5.
9. Edris AA. Controllable var compensator: a potential solution to loadability problem of low capacity power systems. *IEEE Trans Power Syst*. 1987;2(3):561-567.
10. Italian Standard CEI 11-60. Portata al limite termico delle linee elettriche aeree esterne con tensione maggiore di 100 kV. 2<sup>nd</sup> edition, June 2002 (in Italian).
11. Alawar A, Bosze EJ, Nutt SR. A composite core conductor for low sag at high temperatures. *IEEE Trans Power Deliv*. 2005;20(3):2193-2199.

12. CTC Global Corporation. Engineering transmission lines with high capacity low sag ACCC conductors. 2011. Available: [www.ctcglobal.com/wp-content/uploads/2016/05/Engineering\\_Transmission\\_Lines\\_with\\_ACCC\\_Conductor.pdf](http://www.ctcglobal.com/wp-content/uploads/2016/05/Engineering_Transmission_Lines_with_ACCC_Conductor.pdf)
13. Americans for a Clean Energy Grid. High temperature, low sag conductor. 2014. Available: <http://cleanenergytransmission.org/wp-content/uploads/2014/08/High-Temperature-Low-Sag.pdf>
14. Lauria D, Quaia S. An investigation on line loadability increase with high temperature conductors. Proc 6<sup>rd</sup> Int Conf Clean Electrical Power, ICCEP 2017, Santa Margherita Ligure, Italy, June 27-29, 2017.
15. Lauria D, Quaia S. Loadability increase in radial transmission lines through reactive power injection. Proc 6<sup>rd</sup> Int Conf Clean Electrical Power, ICCEP 2017, Santa Margherita Ligure, Italy, June 27-29, 2017.
16. Lauria D, Mazzanti G, Quaia S. Comparative analysis of overhead power transmission lines based on loadability characteristics. Proc 3<sup>rd</sup> Int Conf Clean Electrical Power, ICCEP 2011, Ischia, Italy, June 14-16, 2011:265-271.
17. Billinton R, Kuruganty PRS, Carvalho MF. An approximate method for probabilistic assessment of transient stability. *IEEE Trans Reliabil.* 1979;28(3):255-258.
18. Billinton R, Kuruganty PRS. A probabilistic index for transient stability. *IEEE Trans PAS.* 1980;99(1):195-206.
19. Billinton R, Kuruganty PRS. Probabilistic assessment of transient stability in a practical multimachine system. *IEEE Trans PAS.* 1981;100(7):3634-3641.
20. Billinton R, Kuruganty PRS. Protection system modelling in a probabilistic assessment of transient stability. *IEEE Trans PAS.* 1981;100(5):2163-2170.
21. Chiodo E, Gagliardi F, Lauria D. A probabilistic approach to transient stability evaluation. *IEE Proc Gen, Trans Distrib.* 1994;141(5):537-544.
22. Chiodo E, Lauria D, Mazzanti G, Quaia S. Technical comparison among different solutions for overhead power transmission lines. Proc 20<sup>th</sup> International Symposium on Power Electronics, Electrical Drives, Automation and Motion, Speedam 2010, Pisa (Italy), 14-16 June 2010:68-73.
23. Anders GJ. *Probability Concepts in Electric Power Systems.* New York: John Wiley; 1990.
24. Tiwari SN, Bin Saroor AS. An investigation into loadability characteristics of EHV high phase order transmission lines. *IEEE Trans Power Syst.* 1995;10(3):1264-1270.
25. DuBois EW, Fairman JF, Murphy CM, Martin DE, Ward JB. Extra-long-distance-transmission. *IEEE Trans PAS.* 1961;80(3):1108-1115.
26. El-Metwally MM, El-Emary AA, El-Azab M. A linear programming method for series and shunt compensation of HV transmission lines. *Eur T Electr Power.* 2005;15(2):157-170. <https://doi.org/10.1002/etep.45>